



HAL
open science

One-dimensional discrete formulation of a hygrolock model for wood hygromechanics

Julien Colmars, Frédéric Dubois, Joseph Gril

► **To cite this version:**

Julien Colmars, Frédéric Dubois, Joseph Gril. One-dimensional discrete formulation of a hygrolock model for wood hygromechanics. *Mechanics of Time-Dependent Materials*, 2014, 18, pp.309 - 328. 10.1007/s11043-013-9229-x . hal-01084665

HAL Id: hal-01084665

<https://hal.science/hal-01084665v1>

Submitted on 20 Nov 2014

HAL is a multi-disciplinary open access archive for the deposit and dissemination of scientific research documents, whether they are published or not. The documents may come from teaching and research institutions in France or abroad, or from public or private research centers.

L'archive ouverte pluridisciplinaire **HAL**, est destinée au dépôt et à la diffusion de documents scientifiques de niveau recherche, publiés ou non, émanant des établissements d'enseignement et de recherche français ou étrangers, des laboratoires publics ou privés.

One-dimensional discrete formulation of Hygrolock model for wood hygromechanics

Colmars, J.^{1*}, Dubois, F.², Gril J.¹

¹⁾ *Laboratoire de Mécanique et Génie Civil, LMGC, Université Montpellier 2*

Julien Colmars (corresponding author)

Tel. (+33) 680 966 294 (mobile)

julien.colmars@imelavi.fr

Joseph Gril (scientific contact)

Tel. (+33) 467 143 433

Fax (+33) 467 144 792

joseph.gril@univ-montp2.fr

²⁾ *University of Limoges, GEMH, Bd. Jacques Derche, 19300 Egletons, France*

Frédéric Dubois

Tel. (+33) 555 934 526

Fax (+33) 555 934 501

frederic.dubois@unilim.fr

Abstract: a new 1D discrete formulation of hygrolock models is proposed for modeling wood time-dependent behavior. This discrete formulation is compared to an integral formulation presented in a previously published paper. Simulations with various humidity cycles are performed under constant stress (creep) or constant strain (relaxation) using first a hygrolock spring and then a generalized Kelvin-Voigt model with a time-spectral distribution of hygrolocks springs. The discrete formulation presented here, based on original idea of mixed series/parallel rheological model, is shown to be very practical for implementation in scientific numerical codes. In order to compensate a lack of complete data-set on wood material, a generic time and moisture-dependent material is proposed to compare the various models: this dataset could be re-used in other studies. Finally the relevance of hygrolock models for wood time-dependent behavior is discussed: it appears that hygrolock models suits well to the upper part of wood hygroscopic domain, whereas further hypothesis should be tested for dry domain. A judicious choice in moisture activation of material parameters, combined with the blocking effect of hygrolock, agree with recent experimental results on simplifying the description of so-called ++ effect.

Keywords: hygrolock, wood, mechanosorption, moisture activated creep.

Introduction

Hygromechanical couplings in wood

Wood is a hygroscopic material that exhibits significant mechanical couplings under combined load and humidity changes. Wood relative creep (ratio of time-dependent to elastic strain) increases with moisture content, but during moisture changes under a given load within the elastic domain, wood creeps even more than at the highest moisture condition ever reached during loading. The terms “mechanosorptive effect” or “mechanosorption” introduced by Grossman (1971) are classically used in literature to describe this additional creep (or relaxation) due to moisture variations under stress (resp. imposed strain). This was evidenced experimentally since the 40ies (see comments by Schniewind (1966), Gril (1988)), and later by Armstrong and Kingston (1960). These couplings are of great importance for timber structure prediction, but researchers are still working on finding simple and accurate mathematical solutions to describe this complex behavior.

A large number of rheological models used for modeling mechano-sorptive effect have been developed in the past. The first models were based on a de-coupling between viscoelastic behavior and additional effects affected by the moisture content h and its variation rate $|dh/dt|$. Moisture content of wood is given by the ratio of water mass within the sample (total mass minus mass of dried sample) to the mass of the dried sample.

Leicester (1971) proposed a model which takes a dashpot form whose viscosity η is a moisture content function as described by the following stress-strain expression (1):

$$\eta(h, |\dot{h}|) \frac{d\varepsilon}{dt} = \sigma \quad (1)$$

At constant stress, these models produce an increment of strain under both drying and moistening (because of term $|dh/dt|$); conversely, at constant strain the model produces relaxation under any moisture change. This model also used by Grossman (1971) allowed describing longitudinal creep and relaxation tests on hoop pine timber. In the same way, Rybarczik and Ganowicz (1974) described swelling pressure of wood across the grain (i.e. swelling-induced stress under

constant strain). Later Ranta-Maunus (1975), using various dataset on softwoods, proposed a generic approach of mechanosorption in wood as:

$$d\varepsilon = a\sigma|dh| \quad (2)$$

where a is a material parameters taking different values a^+ and a^- according to the sign of dh . He also stated that specific value a^{++} is needed to describe the so-called “++ effect” when moisture reach the highest level ever under load.

Similar approach was conducted on concrete (Bazant, et al. (1997)) to describe additional creep caused by the decreasing of humidity in the concrete pores due to hydration reaction, see Pickett (1941). In this case the viscosity depends on dh/dt . Modeling both drying and wetting in wood leads to use absolute value $|dh/dt|$, which results mathematically in infinite strain for continuous moisture variation between given upper and lower bounds. For very small but continuous variations of h , this mechano-sorptive behavior does not converge to creep at constant moisture content.

These models have been widely used in wood studies in addition to classical elastic and viscoelastic models, which mean that modeling mechanosorption usually requires more parameters than modeling wood mechanics at constant humidity. In contrast to this, one aim of the hygrolock models showed in this paper will be to rely only on constant moisture behavior to deduce complex behavior at variable humidity; similar approach has been attempted theoretically by Nakano (1999).

Leicester phenomenological model was used both in series for producing non-recoverable mechano-sorptive strain, or associated in parallel to a linear spring to take into account a linear creep limit (see Hunt (1984), Hanhijärvi and Hunt (1998), Montero et al. (2012)). For a larger review on phenomenological models applied to wood material, we recommend following references: Chassagne et al. (2006), Randriambololona (2003), Bou Saïd (2003), Moutee (2006) and Montero et al. (2012) for recent advances in experimental characterization of mechanosorption.

Hygrolock models

Concept of hygrolock was first proposed by Gril (1988) to model mechanosorption in wood. The idea was to create additional deformation by blocking strain (or stress) during drying by using various modeling levels corresponding to moisture content levels.

Dubois et al. (2005) proposed a first numerical formulation of hygrolock spring by using two different behaviors during drying and wetting: during wetting (softening of wood) a simple Hooke law is used whereas during drying (hardening of wood) Bazant law (tangent Hooke law) is preferred; this produces blocking effect during drying as proposed by Gril (1988), but Randriambololona (2003)

showed the difficulties involved when synchronizing these two constitutive laws for moisture content cycles.

Later Husson et al. (2009) developed a second version of hygrolock models involving the principle of internal (or fixed) stresses proposed by Liu (2006). In this case total stress on the material is the sum of mechanical stress (that induces deformation) and fixed stresses (due to rigidity variation during drying) which are stored temporary within the material and show no effect on deformation. The calculations by Husson (2009) for the hygrolock spring led to the following integral form:

$$\varepsilon_e(t) = \int_{0-}^t \frac{1}{k_{\min}(\tau, t)} \cdot \frac{\partial \sigma}{\partial t} d\tau \quad (3)$$

in which $k_{\min}(\tau, t)$ designates the rigidity minimum between times τ and t .

Introducing this mechano-sorptive spring in a generalized Kelvin Voigt (GKV) representation, Dubois et al. (2011) defined a double integral of time and moisture which leads to a complete time-dependent formulation incorporating strain blockings during the drying period as well as memory effects during wetting phases after unloading. Each Kelvin-Voigt body admits the following behavior:

$$\varepsilon(t) = \int_0^t \left[\int_{\tau}^t \frac{1}{\eta(\vartheta)} \cdot \exp^{-\int_{\tau}^{\vartheta} \frac{k_{\min}(\alpha, t)}{\eta(\alpha)} d\alpha} \cdot d\vartheta \right] \cdot \frac{\partial \sigma}{\partial \tau} \cdot d\tau \quad (4)$$

By using incremental formulation deduced from equation (5), Dubois (2012) gave the formulation of a discrete time-dependant behavior including hygrolock effect for implementation in finite element code.

In parallel to this work, we developed another model by using a different physical approach based on moisture levels initially proposed by Gril (1988): unless the basic assumptions are quite different, it will be shown that these different models behave qualitatively and quantitatively the same way under various load configurations.

With the specific aim of comparing various models on the same loading history, we also propose in this paper a method to calculate a complete set of parameters from two creep curves at low and high moisture content, in order to model creep of wood at varying humidity. Finally, we discuss the relevance of such models to describe moisture and time-dependent behavior of wood.

General principles of hygrolock spring

This paper focuses on a one-dimensional approach using a discrete scheme in time and moisture levels. Hygrolock basis is an elastic body (spring) that exhibits a blocking behavior during moisture changes under the highest moisture value ever under load. The schematic representation of the hygrolock unit proposed by Husson (2009) is shown in Figure 1.



Figure 1: symbol for hygrolock spring as proposed by Husson (2009)

Hygrolock models have various objectives in wood material behavior, which will be detailed next. It should for example:

- simplify the ++ effect of mechanosorption, defined by Ranta-Maunus (1975),
- avoid non-thermodynamic behavior of hygro-elastic element,
- be an alternative (or additional solution) to Leicester model,
- generate complex behavior at varying moisture content using only parameters determined at constant humidity.

The following sections will give more details on each point.

Hygrolock for ++ effect

The concept of hygrolock proposed by Gril (1988) reproduces the so-called “++ effect” of mechanosorption defined by Ranta-Maunus (1975). This effect is observable during a creep test under moisture content changes: it consists in a marked increase of the strain to moisture rate ($d\varepsilon/dh$) when moisture content reaches the highest level ever reached under load. Expression (2) is used to describe creep of various softwoods by using 3 parameters a^+ , a^- and a^{++} .

The ++ effect is illustrated on Figure 2a, with the schematic representation proposed by Hunt (1984), where total strain (of creep test) minus free swelling strain (of matched samples) is plotted against moisture content.

The hygro-lock spring as proposed by Gril (1988) blocks strain during drying (-) and moistening (+) phases in order to underline the (++) phases (Figure 2b).

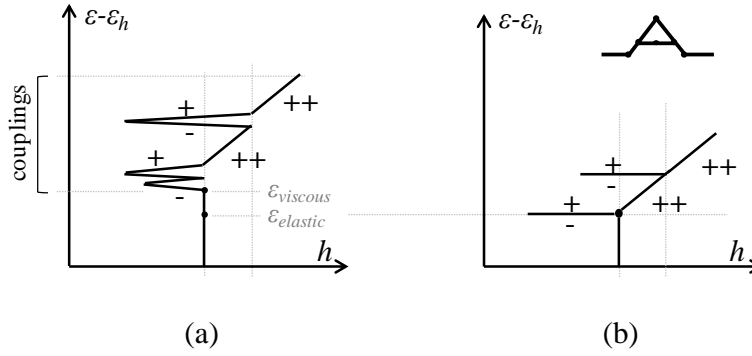


Figure 2: Creep trajectories according to Hunt's representation, giving the total strain (ε) corrected for free swelling strain (ε_h) versus moisture content (h): (a) typical creep response of wood far from creep limit; (b) hygrolock spring behavior; drying phase (-), moistening phases (+) and moistening phases over the highest moisture level ever (++) under load.

Hygrolock as a thermodynamic spring

Another objective of hygrolock spring has been already discussed in details by Husson (2009) and Dubois (2004): it consists in proposing a hygro-elastic body that fulfills the second thermodynamic law during both drying and moistening. Actually a problem is raised by the dependency of elastic rigidity of wood to moisture content. Because rigidity of wood decreases with increasing moisture content (Guitard (1987), Kollmann and Côté (1968)), the minimal hygro-elastic body should recover partly its deformation under drying and constant load: this consequence does not fulfill the second law of thermodynamics (see Chassagne et al. (2006), Randriambololona (2003), Husson (2009), Dubois (2004)) and is never observed experimentally.

The classical solution for modeling strain increase observed in such conditions consists in adding other models in series (Leicester model for example) to the basic linear spring. Another solution is to enhance the formulation of the hygro-elastic elementary body. Hygrolock spring as shown next is thus an enhanced hygromechanical spring, i.e. a self-sufficient model for hygro-elastic behavior. In this paper we show that using the same Hygrolock spring into a Kelvin-Voigt body leads to a satisfactory time-dependent formulation.

Incremental formulation of hygrolock spring

In this paper we model a hygrolock spring as a combination of n Hooke springs. Each spring $k = 1, \dots, n$ stands for a bounded moisture domain, also called "box"

below. Hygroscopic range of wood (dry state $h_0 = 0\%$ to Fiber Saturation Point $h_n \approx 30\%$) is thus divided into n boxes (see Figure 3) ordered by increasing h .

Box k is thus defined as:

$$h \in [h_{k-1}, h_k] = \left[(k-1) \frac{h_n}{n}, k \frac{h_n}{n} \right], k = 1, \dots, n \quad (5)$$

Characteristic moisture content of each box is here chosen to be the mean value $(h_{k-1} + h_k)/2$ of its upper and lower bounds. Spring k is characterized by a constant compliance J_k and exhibits classical linear behavior as defined by (eq.6). As assumed for all wood species and all orthotropic directions, compliance is an increasing function of h ($J_{k+1} > J_k$).

Each box means a range of moisture content, or a level of sorption energy. The repartition of the corresponding sorption sites in the molecular structure is complex and does not fit with either a parallel or a series disposition. Therefore, a mixture of both has been chosen. Total strain E of hygrolock spring is proposed to be the sum of all spring strains (eq.7). The original point is that total stress S will also be the sum of all stresses in each level (eq.8). This choice results in a mixing between series and parallel rheological assembly.

$$\varepsilon_k = J_k \sigma_k \quad 1 \leq k \leq n \quad (6)$$

$$E = \sum_{k=1}^n \varepsilon_k \quad (7)$$

$$S = \sum_{k=1}^n \sigma_k \quad (8)$$

As an alternative choice, we could have defined the stress as the mean box stress or the strain as the mean box strain. In any case, the concept of boxes does not require any physical mechanism to be applicable.

Moisture content at current time will set the so-called “active box”: determination and role of the active box are detailed next. This type of hygrolock model is thus based on the discretization of both time and hygroscopic domain; the latter will impose sometimes the choice of time steps depending on moisture history, which is explained in next section.

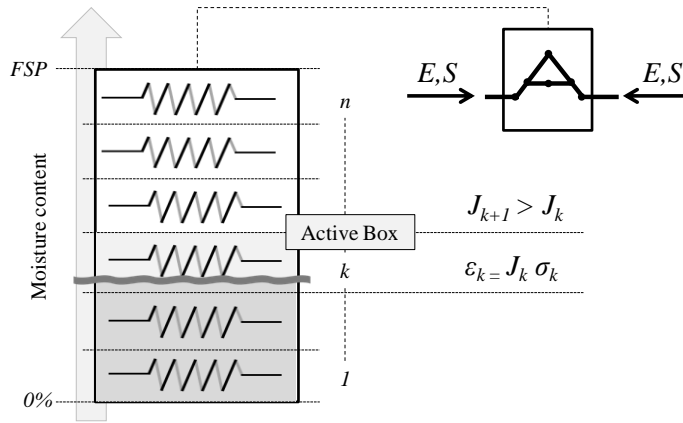


Figure 3: Schematic representation of boxes within a hygrolock spring. The hygroscopic range of wood (from totally dry wood $h_0 = 0$. to fiber saturation point $h_n \approx 0.3$) is divided into n boxes. Current moisture level gives the “active box”. As for all wood species and orthotropic directions, box compliance increases with moisture content.

Moisture event in the hygro-lock

In the following, we use a discrete scheme in time, with time steps Δt^i , $t \in [t^i, t^{i+1}[$. All superscripts i refer to variables at time t^i . Active box at t^i is noted k^i and is given by moisture content h^i . At t^{i+1} active box is k^{i+1} . Thus during time step Δt^i , three different cases might occur: moistening ($k^{i+1} > k^i$), drying ($k^{i+1} < k^i$) or stabilization of moisture content (*statu quo*, $k^{i+1} = k^i$).

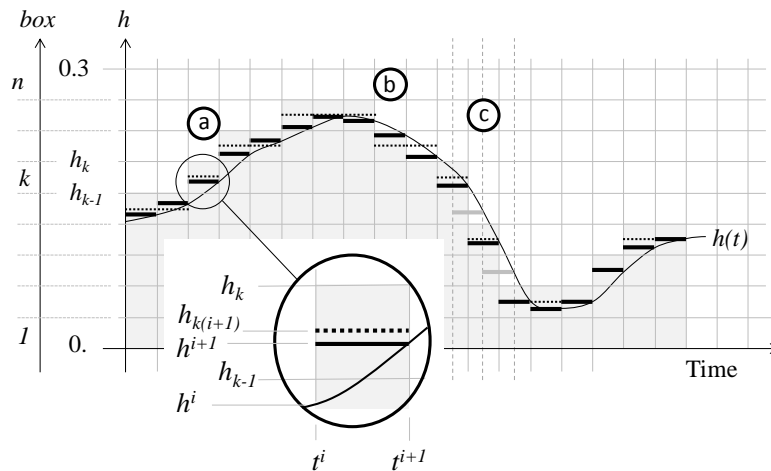


Figure 4: Discretisation of time and moisture along the moisture curve $h(t)$. (a) Moistening with zoom; (b) drying; (c) jump of 2 boxes during Δt . Thick black bars: active moisture content during Δt (which is moisture content at t^{i+1}). Dotted black bars: characteristic moisture $h_{k(i+1)}$ of active box during Δt . Thick gray bars: new active box after interpolation of original data (to avoid jump (c)). Gray vertical bars: coloration from box 1 to active box.

The hygrolock effect presented in this paper is based on stress transfer to subsequent active box when moistening, and stress blocking in original box when drying. Strain variations in hygrolock are directly deduced from stress transfers using expression (7-8).

Whatever the event, only two boxes are put under varying stresses: k^i and k^{i+1} , whereas all other boxes remain in their previous stress-strain state. We further assume that a moisture change does not skip any box, i.e. that $|k^{i+1} - k^i| \leq 1$ (this is guaranteed in numerical code by initial interpolation of input moisture data, see case (c) in Figure 4). Table 1 sums up the three different cases: we define two binary variables, Ψ and Π , which will be used to write hygrolock spring equations whatever the event.

Table 1: description of active boxes for each moisture event during time step.

Case	Ψ	Π	Active box $t(i)$	Active box at $t(i+1)$
Moistening	1	1	k^i	$k^{i+1} = k^i + 1$
Statu quo	0	0	k^i	$k^{i+1} = k^i$
Drying	0	1	k^i	$k^{i+1} = k^i - 1$

The total variation of strain and stress in the hygrolock spring during Δt^i is given for any case (moistening, drying or *statu quo*) by expression (9-10). Note that, in order to improve readability, k^i will be written $k(i)$ when used as subscript.

$$\Delta S = \Delta \sigma_{k(i)} + \Pi \Delta \sigma_{k(i+1)} \quad (9)$$

$$\Delta E = J_{k(i)} \Delta \sigma_{k(i)} + \Pi J_{k(i+1)} \Delta \sigma_{k(i+1)} \quad (10)$$

The general behavior of hygrolock spring during Δt^i will be written using expression (11), where P is a hygro-strain and Q a compliance.

$$\Delta E = P + Q \Delta S \quad (11)$$

In next sections we will identify the expressions of P and Q for each moisture event. Finally, generic expressions of P and Q for any event will be proposed.

Moistening

All following expressions are written for $t \in [t^i, t^{i+1}]$; k^i will be simplified into k in case of no possible mix-up. During moistening phases, we assume that stress

of box k (previous active box) is progressively (linearly) transferred to the new active box $k + 1$:

$$\left. \begin{aligned} \sigma_j(t) &= \sigma_j^i \quad \forall j \neq k, k+1 \\ \sigma_k(t) &= \sigma_k^i \left(1 - \frac{t-t^i}{\Delta t} \right) \\ \sigma_{k+1}(t) &= \sigma_{k+1}^i + (\sigma_k^i + \Delta S) \frac{t-t^i}{\Delta t} \end{aligned} \right\} t^i \leq t \leq t^{i+1} \quad (12)$$

Here we supposed that all external stress ΔS occurring during time step is fully supported by box $k + 1$, in other words that $k + 1$ is the active box during all time step. In case of moistening, this assumption has no consequence on elastic behavior: indeed even if k bears some part of ΔS , it will be transferred later during Δt to $k + 1$ with all other stresses. Strain transfer (eq.13) is directly deduced from linear elastic behavior of each box (eq.6).

$$\left. \begin{aligned} \varepsilon_j(t) &= \varepsilon_j^i \quad \forall j \neq k, k+1 \\ \varepsilon_k(t) &= J_k \sigma_k(t) = J_k \sigma_k^i \left(1 - \frac{t-t^i}{\Delta t} \right) \\ \varepsilon_{k+1}(t) &= J_{k+1} \sigma_{k+1}(t) = \varepsilon_{k+1}^i + J_{k+1} (\sigma_k^i + \Delta S) \frac{t-t^i}{\Delta t} \end{aligned} \right\} t^i \leq t \leq t^{i+1} \quad (13)$$

Total strain in the hygrolock spring (eq.14) is obtained by adding strain changes in boxes k^i and k^{i+1} , and all the possible internal strains stored in the other boxes.

$$\begin{aligned} E(t) &= \varepsilon_k(t) + \varepsilon_{k+1}(t) + \left[\sum_{j \neq k; k+1} \varepsilon_j^i \right] \\ &= J_k \sigma_k(t) + J_{k+1} \sigma_{k+1}(t) + \left[\sum_{j \neq k, k+1} J_j \sigma_j^i \right] \\ &= E^i + \left[(J_{k+1} - J_k) \sigma_k^i + J_{k+1} \Delta S \right] \frac{t-t^i}{\Delta t} \end{aligned} \quad (14)$$

By derivation of expression (14), we confirm that total strain rate is constant under the assumption of linear external stress evolution. Then we deduce the set of equations (17) giving ΔE during moistening:

$$\left. \begin{aligned} \Delta E &= P + Q\Delta S \\ P &= (J_{k+1} - J_k)\sigma_k^i \\ Q &= J_{k+1} \end{aligned} \right\} (15)$$

Expression (15) is rewritten in a more general form (eq.16), to be used whatever the moisture event.

$$\left. \begin{aligned} \Delta E &= P + Q\Delta S \\ P &= (J_{k(i+1)} - J_{k(i)})\sigma_{k(i)}^i \\ Q &= J_{k(i+1)} \end{aligned} \right\} (16)$$

Drying

During drying hygrolock spring blocks the stress in the upper box. Then stresses are not transferred from box k^i to box k^{i+1} . Thus the only variation in stress state is due to external increment ΔS (eq.17). Once again, we suppose that external stress is fully supported by $k^{i+1} = k^i - 1$.

$$\sigma_{k-1}(t) = \sigma_{k-1}^i + \frac{\Delta S}{\Delta t}(t - t^i) \quad (17)$$

In expression (17), σ_{k-1}^i is often equal to 0, because all stresses would have been transferred in σ_k^i during previous moistening; exception occurs ($\sigma_{k-1}^i \neq 0$) if simulation has started with an initial stress state.

Expression (17) is then injected into (6) to give the expression of strain in the new active box:

$$\varepsilon_{k-1}(t) = J_{k-1}\sigma_{k-1}(t) = J_{k-1}\left(\sigma_{k-1}^i + \frac{\Delta S}{\Delta t}(t - t^i)\right) = \varepsilon_{k-1}^i + J_{k-1}\frac{\Delta S}{\Delta t}(t - t^i) \quad (18)$$

Whereas former active box doesn't see any change, reproducing the blocking effect.

$$\varepsilon_k(t) = J_k\sigma_k(t) = J_k\sigma_k^i \quad (19)$$

The total strain is deduced from expressions (18-19):

$$E(t) = J_k \sigma_k + J_{k-1} \sigma_{k-1} + \left[\sum_{j \neq [k-1;k]} J_j \sigma_j^i \right] = E^i + J_{k-1} \frac{\Delta S}{\Delta t} (t - t^i) \quad (20)$$

Once again, total strain rate on the hygrolock spring is constant. As for moistening, we provide general behavior under the (eq.11) form.

$$\left. \begin{aligned} \Delta E &= P + Q \Delta S \\ P &= 0 \\ Q &= J_{k(i+1)} \end{aligned} \right\} (21)$$

Statu quo

Statu quo is the simplest case: the active box bears the total stress increment ΔS (eq.22) and no stress transfer occurs:

$$\sigma_k(t) = \sigma_k^i + \frac{\Delta S}{\Delta t} (t - t^i) \quad (22)$$

$$\varepsilon_k(t) = J_k \sigma_k^i + J_k \frac{\Delta S}{\Delta t} (t - t^i) \quad (23)$$

$$E(t) = J_k \sigma_k + \left[\sum_{j \neq k} J_j \sigma_j^i \right] = E^i + J_k \frac{\Delta S}{\Delta t} (t - t^i) \quad (24)$$

which leads obviously to classical Hookean behavior:

$$\left. \begin{aligned} \Delta E &= P + Q \Delta S \\ P &= 0 \\ Q &= J_{k(i)} = J_{k(i+1)} \end{aligned} \right\} (25)$$

Drying and *statu quo* are equivalent in terms of stress-strain relation; they are not from internal stress transfer point of view (see expression (27) below).

General behavior or hygrolock spring

To sum up we give hygrolock spring constitutive law whatever the event (eq.26), by using parameter Ψ , defined in Table 1, which is equal to 1 in case of moistening, 0 otherwise.

$$\left. \begin{aligned} P &= \Psi(J_{k(i)} - J_{k(i+1)})\sigma_{k(i)}^i \\ Q &= J_{k(i+1)} \end{aligned} \right\} (26)$$

We also give expression for the stress transfers (eq.27) using parameter Π equal to 0 during *statu quo*, and 1 otherwise:

$$\left. \begin{aligned} \sigma_{k(i+1)}^{i+1} &= \sigma_{k(i+1)}^i + \Psi \sigma_{k(i)}^i + \Delta S \\ \sigma_{k(i)}^{i+1} &= (1 - \Psi)\sigma_{k(i)}^i \end{aligned} \right\} \text{if } \Pi \neq 0 \quad (27)$$

Note that restriction of expression (27) in the case of *statu quo* needs to be correctly implemented in calculation program because $k^i = k^{i+1}$.

Simulations of hygrolock spring

The previous equations have been implemented into the interpreted programming environment Scilab (www.scilab.org). A simulation test shown on Figure 5 is commented next. Stress and moisture content cycling are imposed, and strain is calculated. Significant events occur during the loading history, they are numbered from 1 to 9 on Figure 5:

1. HygroLock spring is wetted under load, compliance and strain increase,
2. Spring is dried, compliance decreases but strain is blocked,
3. Higher moistening leads to strain increase,
4. Spring is unloaded at low humidity, remaining strain has been blocked during the previous drying,
5. New moistening phases allow to recover strain completely,
6. Now spring is loaded wet,
7. Unloading at dry state ; again strain has been blocked in the upper boxes,
8. Small moistening allows recovering partly residual strain,
9. A new moistening to the condition when loaded allows complete recovery.

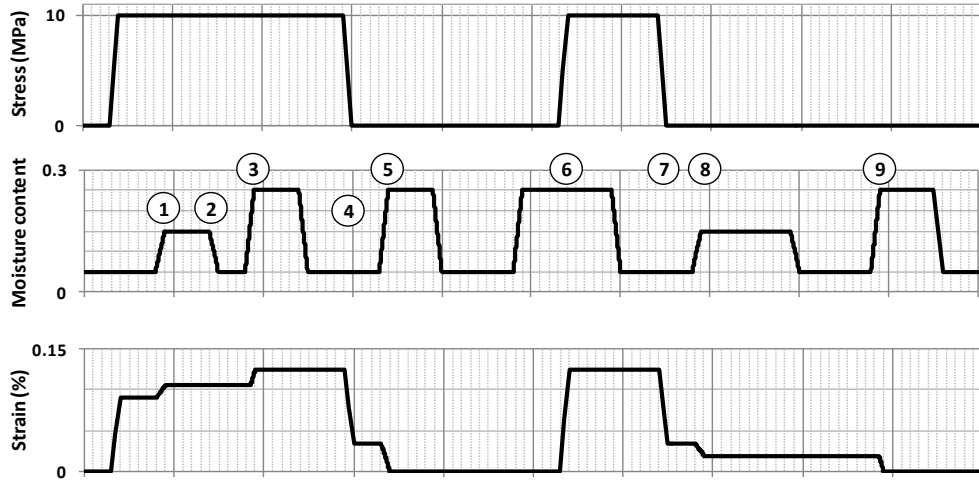


Figure 5 : simulation test of the hygrolock spring. Stress and moisture content cycling is imposed, strain is calculated. Various significant events are numbered from 1 to 9.

Incremental formulation of a hygrolock Kelvin-Voigt body

Here we explain the behavior of a hygrolock spring when assembled in parallel to a Newtonian dashpot, in order to form a hygrolock Kelvin-Voigt body (Figure 6). The Kelvin-Voigt body is put under stress σ and strain ε ; E and S are still the global strain and stress of the hygro-lock spring. In this specific case $\varepsilon = E$.

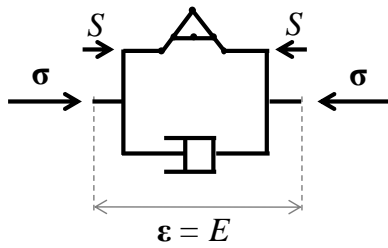


Figure 6: Hygrolock Kelvin-Voigt body, ε and σ are external strain and stress on the body. E and S are the external strain and stress applied on the hygrolock spring.

Expression (28) reminds the general equation of the Kelvin-Voigt body.

$$\sigma(t) = S(t) + \eta \dot{\varepsilon}(t) \quad (28)$$

We assume that external stress σ varies linearly during time step Δt .

$$\sigma(t) = \sigma^i + \frac{\Delta\sigma}{\Delta t}(t - t^i) \quad , t^i \leq t \leq t^{i+1} \quad (29)$$

This allows solving easily the differential equation (28). The solution is detailed next for each moisture event.

Moistening

Stress transfers in the hygro-lock spring remain the same that in elastic case (see expression (27)). General equation (28) of the Kelvin-Voigt body is first multiplied by J_{k+1} to obtain:

$$\tau \dot{\boldsymbol{\varepsilon}}(t) + J_{k+1} S(t) = J_{k+1} \boldsymbol{\sigma}(t) \quad (30)$$

where $\tau = J_{k+1} \eta$ is a characteristic time of the Kelvin-Voigt body.

Then expression of $S(t)$ is modified to make $\boldsymbol{\varepsilon} = E$ appear into the ordinary differential equation (ODE). According to characteristic equations of hygro-lock spring (eq.6-8), we can write:

$$J_{k+1} S(t) = J_{k+1} \sum_{j=1}^n \sigma_j(t) = J_{k+1} \left(\sum_{j \neq k, k+1} \sigma_j^i + \sigma_k(t) + \sigma_{k+1}(t) \right) \quad (31)$$

Whereas expression of $E(t)$ gives:

$$E(t) = \sum_{j=1}^n J_j \sigma_j(t) = \sum_{j=1}^n \frac{J_j}{J_{k+1}} J_{k+1} \sigma_j(t) \quad (32)$$

Subtraction of expressions (31) and (32) gives:

$$\begin{aligned} J_{k+1} S(t) - E(t) &= \sum_{j=1}^n \left(1 - \frac{J_j}{J_{k+1}} \right) J_{k+1} \sigma_j(t) \\ &= \sum_{j \neq k, k+1} \left(\frac{J_{k+1} - J_j}{J_{k+1}} \right) J_{k+1} \sigma_j^i + \frac{J_{k+1} - J_k}{J_{k+1}} J_{k+1} \sigma_k(t) \end{aligned} \quad (33)$$

This last expression is used to modify the ODE (30):

$$\begin{aligned} \tau \dot{\boldsymbol{\varepsilon}}(t) + \boldsymbol{\varepsilon}(t) &= J_{k+1} \boldsymbol{\sigma}^i + J_{k+1} \frac{\Delta \boldsymbol{\sigma}}{\Delta t} (t - t^i) - \sum_{j=1}^n (J_{k+1} - J_j) \sigma_j^i + (J_{k+1} - J_k) \sigma_k^i \frac{t - t^i}{\Delta t} \\ &= J_{k+1} \boldsymbol{\sigma}^i + J_{k+1} \frac{\Delta \boldsymbol{\sigma}}{\Delta t} (t - t^i) - J_{k+1} S^i + \boldsymbol{\varepsilon}^i + (J_{k+1} - J_k) \sigma_k^i \frac{t - t^i}{\Delta t} \end{aligned} \quad (34)$$

which is rewritten into the general form:

$$\left. \begin{aligned} \tau \dot{\boldsymbol{\varepsilon}}(t) + \boldsymbol{\varepsilon}(t) &= C + D(t - t^i) \\ C &= J_{k+1}(\boldsymbol{\sigma}^i - S^i) + \boldsymbol{\varepsilon}^i \\ D &= J_{k+1} \frac{\Delta \boldsymbol{\sigma}}{\Delta t} + (J_{k+1} - J_k) \frac{\boldsymbol{\sigma}_k^i}{\Delta t} \end{aligned} \right\} \quad (35)$$

Solution of equation (35) is given by:

$$\boldsymbol{\varepsilon}(t) = \left(1 - e^{-\frac{t-t^i}{\tau}} \right) (C - D\tau) + D(t - t^i) + \boldsymbol{\varepsilon}^i e^{-\frac{t-t^i}{\tau}} \quad (36)$$

General expression of $\Delta \boldsymbol{\varepsilon} = \boldsymbol{\varepsilon}^{i+1} - \boldsymbol{\varepsilon}^i$ is thus found to be:

$$\left. \begin{aligned} \Delta \boldsymbol{\varepsilon} &= \varphi (C - \boldsymbol{\varepsilon}^i) + \chi D \Delta t \\ \varphi &= 1 - e^{-\frac{t-t^i}{\tau}} \\ \chi &= 1 - \frac{\varphi}{\Delta t / \tau} \end{aligned} \right\} \quad (37)$$

We finally get expression (38) to describe the general behavior of hygro-lock Kelvin-Voigt body in case of moistening.

$$\left. \begin{aligned} \Delta \boldsymbol{\varepsilon} &= P + Q \Delta \boldsymbol{\sigma} \\ P &= \varphi (\boldsymbol{\sigma}^i - S^i) + \chi (J_{k(i+1)} - J_{k(i)}) \boldsymbol{\sigma}_k^i \\ Q &= \chi J_{k(i+1)} \end{aligned} \right\} \quad (38)$$

Drying (or *statu-quo*)

Again, expressions of stress transfers are taken from hygro-lock spring (eq.27). General equation (28) of the Kelvin-Voigt body is now multiplied by J_{k-1} to obtain:

$$\tau' \dot{\boldsymbol{\varepsilon}}(t) + J_{k-1} S(t) = J_{k-1} \boldsymbol{\sigma}(t) \quad (39)$$

where $\tau' = J_{k-1}\eta$ is a new characteristic time. We assume next that $\tau = \tau'$, i.e that viscosity varies together with compliance: further explanations are given in the following. Using the same calculation steps, the ODE is changed into:

$$\left. \begin{aligned} \tau \dot{\boldsymbol{\varepsilon}}(t) + \boldsymbol{\varepsilon}(t) &= C + D(t - t^i) \\ C &= J_{k+1}(\boldsymbol{\sigma}^i - S^i) + \boldsymbol{\varepsilon}^i \\ D &= J_{k+1} \frac{\Delta \boldsymbol{\sigma}}{\Delta t} \end{aligned} \right\} (40)$$

Solution of the ODE (eq.37) is used again to provide the drying behavior of hygrolock Kelvin-Voigt unit:

$$\left. \begin{aligned} \Delta \boldsymbol{\varepsilon} &= P + Q \Delta \boldsymbol{\sigma} \\ P &= \varphi(\boldsymbol{\sigma}^i - S^i) \\ Q &= \chi J_{k(i+1)} \end{aligned} \right\} (41)$$

The same expression is found for the *statu quo* case. However actualization of stresses within the boxes is slightly different (see expression (27)).

General behavior of hygrolock Kelvin-Voigt body

Expression (42) gives the general equation of the hygrolock Kelvin-Voigt unit to be implemented in numerical code.

$$\left. \begin{aligned} \Delta \boldsymbol{\varepsilon} &= P + Q \Delta \boldsymbol{\sigma} \\ P &= \varphi(\boldsymbol{\sigma}^i - S^i) + \Psi \chi (J_{k(i+1)} - J_{k(i)}) \boldsymbol{\sigma}_k^i \\ Q &= \chi J_{k(i+1)} \end{aligned} \right\} (42)$$

Note that internal stresses should be correctly updated during calculation, by using the same equations as for hygrolock spring (eq.27).

Theoretical material for simulations

Hygrolock simulations were performed with two different models: the formulation described in Dubois et al. (2011) (integral method) and the one presented in this paper (discrete method or box method). Wood modeling requires a large number of material parameters: variability of natural material, orthotropy, time-dependence and moisture related behavior make it very difficult to obtain consistent experimental parameters. In order to compare these simulations over a

large range of humidity levels and times, a theoretical material is here proposed for simulation purpose; suitability of this data set is assessed by presenting a literature review on time-dependent effects in wood. Another method found in literature consists in using up-scaling homogenization methods to provide a generic orthotropic time-dependent behavior (Eitelberger 2012, De Borst (2012)). Hygrolocks models need only to be fitted on viscous behavior at constant humidity (for at least two different moisture levels); complex behavior at varying humidity is directly deduced from the hygrolock formulation, without further parameters. Thus we propose a theoretical material defined by a series of creep curves given by power laws. Hygrolock model parameters is calculated by fitting the model on the creep curves over a time range of 1 to 8 of log(time in sec). We give reference parameters for two anatomical directions, one is the longitudinal direction (L), i.e. fibers direction in wood, and the second one is a mean transverse (TR) behavior (for mean radial and tangential anatomical directions of wood). Elastic rigidity (one over compliance) at reference moisture content $h = 0.12$ are chosen to be 10 GPa for L, and ten times lower in TR (1 GPa); these elastic parameters are moisture-dependent, according to expression (43) proposed by Guitard (1987).

$$\frac{1}{J^X}(h) = \frac{1}{J_{12\%}^X} (1 - \lambda^X (h - 0.12)) \quad (43)$$

where superscript X stands for the anatomical direction (L or TR), and $h \in [0, 0.3]$ is the moisture content of wood. The rigidity dependence to moisture parameters ($\lambda^L = 1.5$ and $\lambda^{TR} = 3.0$ [% strain / % moisture content]), are also given in Guitard (1987).

We define two reference creep curves by using 2-parameters power laws:

$$J(t > 0) = J(t = 0) \left(1 + \left(\frac{t}{\tilde{\tau}} \right)^p \right) \quad (44)$$

where $J(t = 0)$ is the instantaneous compliance, p and $\tilde{\tau}$ are 2 parameters defining the time-dependent behavior. Power laws were shown to be suitable for describing wood creep over a large range of directions, moisture content, and time (see Bardet and Gril (2002), Dlouha et al.(2009)), with m values around 0.1-0.4 (Dhoula et al. (2008) (2009)).

We give two reference curves for each anatomical direction, one at low moisture content (0.05) and one at very high moisture content (0.25) to cover common values of moisture content. Table 2 gives all parameters for the reference curves shown in Figure 8. As shown in the literature (Gril et al. (2004), Dhoula et al. (2009)) value of parameters p and $\tilde{\tau}$ decrease with moisture content.

Table 2: theoretical parameters for creep power law at two different moisture content level and anatomical directions.

	Longitudinal		TRansverse	
h	0.05	0.25	0.05	0.25
$1/J$ [MPa]	11050	8050	1210	610
J [MPa ⁻¹]	9.0497E-05	1.2422E-04	8.2644E-04	1.6393E-04
p	0.3	0.15	0.2	0.15
$\tilde{\tau}$ [sec]	1E+07	1E+05	1E+07	1E+05

The hygrolock model used next leans on a hygrolock Generalized Kelvin-Voigt model (GKV), with parameters fitted on the previously given creep curves. The 1D GKV model used here consists of a series of: a hygrolock spring of compliance distribution \mathbf{J}_0 and a series of $m = 8$ Kelvin-Voigt bodies of characteristic times τ_j equally spaced in log time scale from 10 sec to 3 years (1 to 8 in log scale) (see eq.46), associated with delayed compliances distribution $\mathbf{J}_j, j = 1, \dots, m$. It (GKV) is represented in Figure 7.

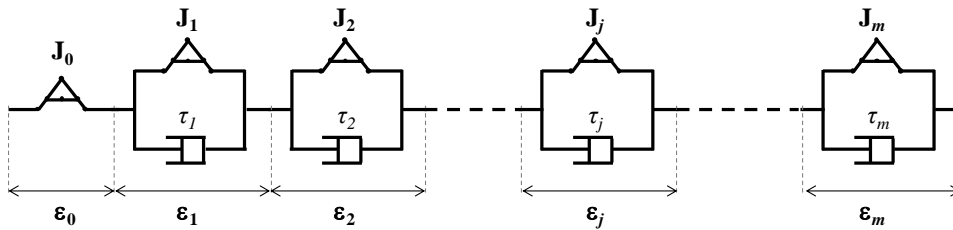


Figure 7: Hygrolock Generalized GKV: hygrolock spring of compliance distribution \mathbf{J}_0 is associated in series with m hygrolock Kelvin-Voigt bodies of compliances distribution \mathbf{J}_j and characteristic time τ_j .

The compliances of our GKV model are not independent variables: a good approximation of the power-law creep response is given by a GKV with a series of viscous compliances J_j that fulfill expression (45).

$$\log(\mathbf{J}_j) = \alpha \cdot \log(\tau_j) + \beta \quad (45)$$

with:

$$\log(\tau_{j+1}/\tau_j) = 1 \quad (46)$$

and where α and β are two linear functions of h , identified at a given humidity:

$$\alpha = \alpha_1 h + \alpha_2 \quad (47)$$

$$\beta = \beta_1 h + \beta_2 \quad (48)$$

Here α and β were calculated at $h = 0.05$ and $h = 0.25$ by best fitting of GKV with reference power laws (by simulating simple creep test at constant humidity). Then coefficients $\alpha_1, \alpha_2, \beta_1, \beta_2$ are simply calculated with equations (47,48). The whole procedure gives all creep parameters at any moisture content between 0.05 and 0.25. All coefficients are summarized in Table 3. Note that all τ_j are considered to be constant for a given Kelvin-Voigt unit: according to expressions (30) and (39), it implies that viscosity η is a function of moisture content, and varies with active box; then the dashpot should also consist in several boxes with viscosities $\eta_k, k = 1, \dots, n$. Since τ_j is constant, apparent characteristic time $\tilde{\tau}$ (time to double the elastic compliance) of equivalent power law decreases with increasing of moisture content (cf. Table 2 and Figure 8). Thus for a given Kelvin-Voigt body, rigidity and viscosity are equally modified by humidity. Alternative (equivalent) formulations with characteristic times modified by humidity would be possible, but this was not the choice made here.

To summarize: from two theoretical creep power-laws at low (0.05) and high (0.25) moisture content, a complete material behavior formulation based on the hygrolock GKV model is determined at any moisture content level. Creep response of such model at intermediate moisture levels is shown on Figure 8. In order to discuss the relevance of this theoretical material for creep modeling, we show on Figure 9 the relative delayed compliance $J(t)/J(t=0)$ against moisture content. As shown by experimental results of Schniewind (1966), Nakano (1999) and Matar (2003), longitudinal relative compliance increases with humidity, and this effect is amplified by time. After 1 day, our material model exhibits relative creep of 1.4 at air-dry condition ($h = 0.12$). At very high moisture content, relative creep at 1 day is around 2.0.

Small corrections could be done on all parameters to fit better a given wood material, but we have here a consistent generic set of time-dependent parameters for L and TR directions to perform numerical simulations and compare different models.

Table 3: Parameters for moisture-time-dependent behavior of hygrolock GKV model at variable moisture content, obtained by fitting it on two reference creep curves (power law).

	Longitudinal	TRansverse
α_1	-0.9624	-0.3574

α_2	0.3386	0.1873
β_1	7.3804	4.5136
β_2	-6.7276	-4.7405

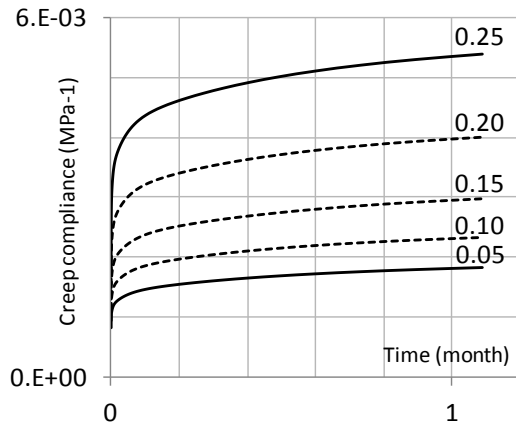


Figure 8: Reference creep curves at 5% and 25% moisture content (plain lines) and calculated creep curves of a hygrolock GKV model with parameters of Table 3 at 10, 15 and 20% moisture content for transverse direction.

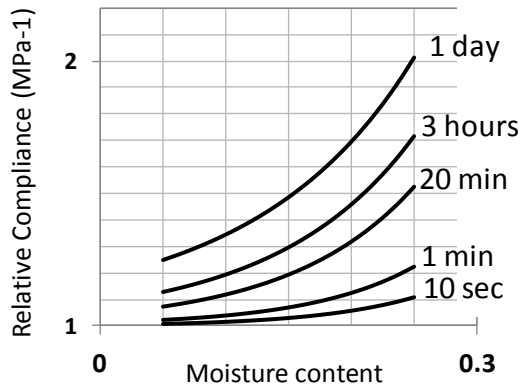


Figure 9: Relative creep compliance $J(t)/J(t=0)$ versus moisture content (0.05-0.25) for longitudinal direction at different times; simulation results using parameters of Table 2 and Table 3.

Simulations

Stress-strain-moisture cycle

Various simulations have been performed using both the formulation presented in this paper and the integral method described in Dubois (2012), using same input data (Table 2-3) and constant time step of 300 seconds.

A theoretical creep test simulation at varying moisture content is shown on Figure 10. The two models give very similar results, but small discrepancies might occur for hazardous choice of moisture boxes, as shown on strain curve from Figure 10. For instance, if active box is not perfectly centered around the current value of moisture content at any time, then the solution given by discrete model slightly moves away from integral model. This is the consequence of regular division of hygroscopic range of wood into n boxes.

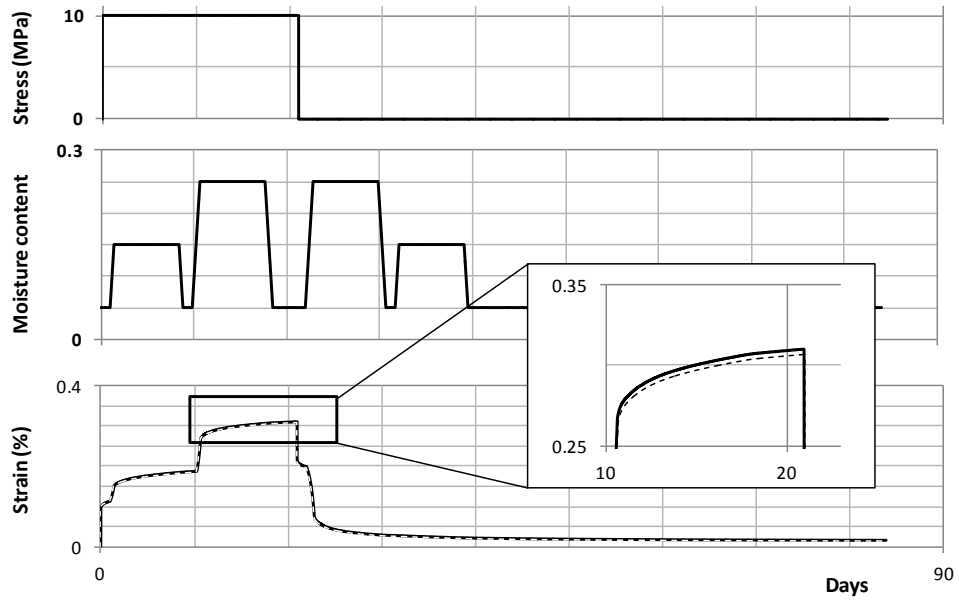


Figure 10: Strain response of hygrolock GKV model to stress-moisture cycling; discrete hygrolock model based on arbitrary chosen moisture boxes (plain curve) and integral method by Dubois (2012) (dashed line).

Mixing parallel and series configuration (eq.7,8) is here of great interest. The general equation (11) can be rewritten in a reciprocal form:

$$\Delta\sigma = Q^{-1}P + Q^{-1}\Delta\varepsilon \quad (49)$$

where $Q^{-1}P$ is a hygroscopic pre-stress and Q^{-1} the rigidity, which allows to simulate also time-dependent relaxation test as shown in Figure 11. Again, the two models give very similar results. This last result was not so obvious considering that discrete hygrolock spring has been built by reallocating stresses between the boxes.

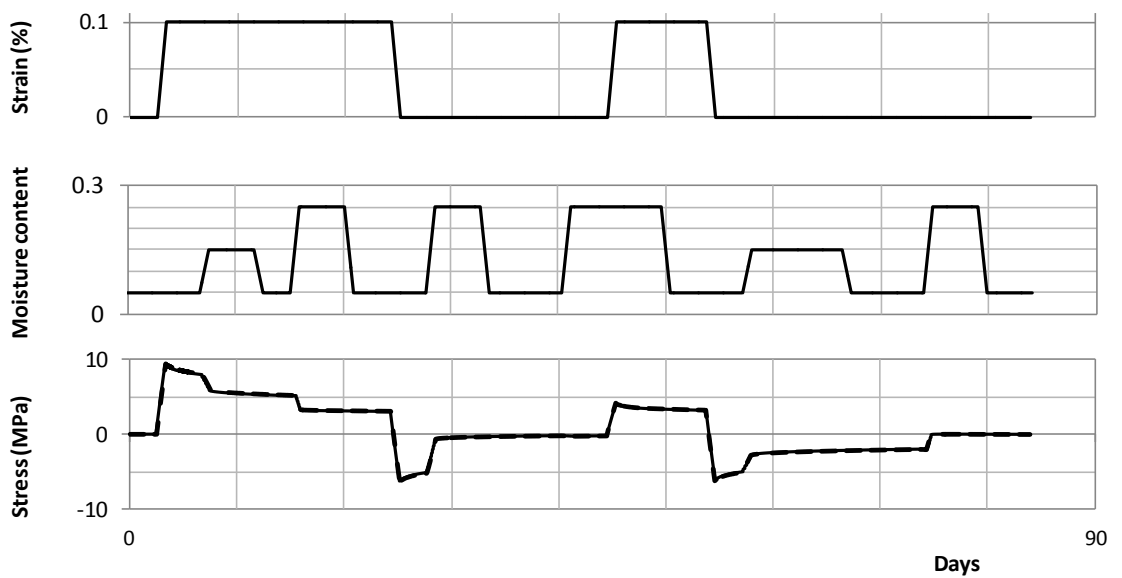


Figure 11: relaxation tests at varying moisture content for a hygrolock GKV model; (plain curve) and integral method by Dubois (2012) (dashed line); maximum difference between the two curves less that 0.2%

Conclusion

For modeling mechanosorption in wood, models using varying compliance with $|dh/dt|$ have been widely used: although they are quite convenient in terms of programming, they require additional parameters and they produce infinite strain during creep when $\sum |dh/dt|$ tends to $+\infty$.

The hygrolock model presented in this paper aims at giving a stable formulation for the mechanical behavior of wood at varying moisture content. The use of

moisture content levels as proposed by Gril (1988) allowed a formulation with internal variables: this is of particular interest for not having to store the entire moisture history for knowing the highest moisture content under load (see Dubois (2005)).

The discrete hygrolock model proposed here relies on the use of “boxes” corresponding to moisture levels, and on stress transfer between boxes according to external moisture events. The originality of considering both total strain and total stress in the hygrolock as the sum of strain (resp. stress) of each box led to a complete formulation for creep and relaxation. Although the fundamental hypotheses are quite different, the discrete model gives very similar results compared to the previous formulation by Dubois (2012).

In order to implement the present hygrolock model, one should focus on equations (26,27) for the hygro-elastic part, and (42,27) for the time-dependent GKV model. The response of the discrete model slightly depends on the box number, but appears to be robust: unlike the Leicester model, hygrolock model tends to viscoelastic creep when the amplitude of moisture variations tends to zero. The GKV model has also been used to simulate a time-dependent relaxation test with complex moisture variations. In the future this model could be used to simulate mixed conditions (alternate strain and stress control) likely to occur in wooden assemblies.

The hygrolock time-dependent model presented in this paper seems to be very interesting for wood at high humidity. Indeed, Montero (2012) showed that samples which creep at high humidity level and samples subjected to previous moisture cycling converge to the same creep limit. In other words for high moisture levels, mechano-sorptive behavior doesn't give much additional deformation compared to stable viscoelastic response. However a “++ effect”, i.e. an increase of apparent strain rate during new moistening, can still be observed during experimentation on wood. We interpret this phenomenon as the combination of two effects: the first is due to blocking/releasing of hygrolock during new moistening, and the second is the dependency of delayed compliance to moisture content which has been shown to be non-linear with moisture content. On the other hand it is quite evident that hygrolock model is not sufficient for low humidity domain where we still observe a significant amount of additional mechano-sorptive deformation compared to creep at constant humidity. This

strong difference between the two domains (high and low moisture content) evidenced by Montero et al. (2012), is a real difficulty for models to fit both: while Leicester model seems to reproduce the additional strain at low moisture content, hygrolock model seems to fit better the high moisture content domain. Our interpretation is that wet state of wood is closer to the initial state within the tree, whereas in dry state wood exhibits specific behavior, maybe due to a specific initial state: the presence of high internal stresses initially blocked in dry wood could be a reason for significant additional creep to occur during the following moisture variations. Conversely, in the wet domain, wood is most probably closer to an initial free of stress state, for which our hygrolock model is qualitatively satisfactory.

In near future hygrolock formulation could be used to model the effect of high internal stresses as initial conditions for dry wood.

Aknowledgments: The authors gratefully acknowledge the financial support of the Austrian Research Promotion Agency (FFG, project number 815234/12791) and the wood industry partnership “Building with Wood” within CEI-Bois for supporting this research work within project “ MechWood ”. COST (European Cooperation in Science and Technology) action IE0601 (Wood sciences for cultural heritage) is also greatly acknowledged for having supported cooperation among authors of this paper and others researchers. Special thanks to Cédric Montero for his fruitful comments.

Bibliography

Bardet, S. et Gril, J. (2002) Modelling the transverse viscoelasticity of green wood using a combination of two parabolic elements, *Comptes rendus mécanique*, vol. 330, p.549-556.

Bazant, Z. P., Baweja, S. et F-J, U. (1997) Microprestress-Solidification Theory for Concrete Creep. Part I : aging and drying effects, *Journal of engineering Mechanics*.

Bazant, Z. P. (1985) Constitutive equation of wood at variable humidity and temperature, *Wood Sci. Technol*, vol. 19, p.159-177.

Bou Saïd, E. (2003), PhD thesis, Contribution à la modélisation des effets différés du bois et du béton sous conditions climatiques variables. Application aux structures mixtes bois-béton., Institut National des Sciences Appliquées (INSA) de Lyon.

Chassagne, P., Bou-Saïd, E., Jullien, J.F., Gallimard, P. (2006) Three Dimensional Creep Model for Wood Under Variable Humidity-Numerical Analyses at Different Material Scales, *Mechanics of Time-Dependent Materials*, vol. 9, p.203–223.

Colmars, J. (2011), PhD thesis, *Hygromécanique du matériau bois appliquée à la conservation du patrimoine culturel : étude sur la courbure des panneaux peints*, Université Montpellier 2

De Bors K and al. (2012) Mechanical characterization of wood: an integrative approach ranging from nanoscale to structure, *Computers and structures*,
<http://dx.doi.org/10.1016/j.compstruc.2012.11.019>

Dlouhá (2009), On the time-temperature equivalency in green wood: characterization of viscoelastic properties in longitudinal direction, *Holzforshung*, vol.63, p.327-333.

Dlouhá (2008), Evidence and modeling of physical aging in green wood, *Rheologica Acta*, vol. 48 (3), p.333-342.

Dubois, F., Randriambololona, H., Petit, C. (2005) Creep in Wood Under Variable Climate Conditions: Numerical Modeling and Experimental Validation, *Mechanics of Time-Dependent Materials*, Springer Netherlands, vol. 9(2), pages 173-202.

Dubois, F., Husson, J.M, Sauvat, N., Manfoumbi, N. (2012) Modeling of the viscoelastic mechano-sorptive behavior in wood, *Mechanics of Time-Dependent Materials*, vol. 16(4), p.439-460.

Eitelberger, J., Bader, T.K, de Borst, K., Jäger, A. (2012) Multiscale prediction of viscoelastic properties of softwood under constant climatic conditions, *Computational Materials Science*, vol. 55, p.303-312.

Gril, J. (1988), PhD thesis, *Une modélisation du comportement hygro-rhéologique du bois à partir de sa microstructure*, Université Paris 6.

Gril, J., Hunt, D., Thibaut, B. (2004), Using wood creep data to discuss the contribution of cell-wall reinforced material, *C.R. Biologie*, vol.327, p.881-888.

Grossman, P.U.A (1971), The use of Leicester's "rheological model for mechano-sorptive deflection of beams", *Wood Science and Technology*, vol. 5,p.232-235.

Guitard, D. (1987) *Mécanique du matériau bois et composites*, Cépaduès-Editions, 2 85428 152 7.

- Leicester, R. H. (1971) A rheological model for mechano-sorptive deflections of beams, *Wood Science and Technology*, vol. 5, p.211-220.
- Hunt, D. G. (1984) Creep Trajectories for Beech during Moisture Changes under Load, *Journal of Materials Science*, vol. 19, p.1456-1467.
- Husson, J.M (2009) PhD thesis, Loi de comportement viscoélastique avec effet mémoire : application à la mécanosorption dans le bois, Université de Limoges.
- Husson, J.M., Dubois F., Sauvat N (2009), Elastic response in wood under moisture content variations: analytic development, *Mechanics of Time Dependent Materials*, doi: 10.1007/s11043-009-9104-y, MTDM149.2
- Husson, J.M., Dubois F., Sauvat N (2011), A finite element model for shape memory behavior, *Mechanics of Time Dependent Materials*, doi: 10.1007/s11043-011-9134-0, 2011
- Liu, Y., Gal, K., Dunn, M.L., Greenberg, A.R., Diani, J., (2006) Thermomechanics of shape memory polymers: Uniaxial experiments and constitutive modeling. *International Journal of Plasticity*. 22, 279–313.
- Montero, C., Gril, J., Legeas, C., Hunt, D., Clair, B. (2012) Influence of hygromechanical history on the longitudinal mechanosorptive creep of wood, *Holzforschung*, DOI vol. 66, 757-764, doi: <http://dx.doi.org/10.1515/hf-2011-01740174>
- Moutee, M. (2006), PhD thesis, Modélisation du comportement mécanique du bois au cours du séchage, Université Laval.
- Nakano, T. (1999) Analysis of creep of wood during water adsorption based on the excitation response theory, *Journal of Wood Science*, vol. 45, p.19-23.
- Pickett, G. (1942) The effect of change in moisture content on the creep of concrete in sustained load, *ACI*, vol. 38, p.333-355.
- Randriambololona, H. (2003), PhD thesis, Modélisation du comportement différé du bois en environnement variable, Université de Limoges.
- Ranta-Maunus, A. (1975) The viscoelasticity of wood at varying moisture content, *Wood Science and Technology*, vol. 9, p.189-205.
- Rybarczik, W., Ganowicz, R. (1974) A Theoretical Description of the Swelling Pressure of Wood, *Wood Science and Technology*, vol. 8, p.233-241.

Schniewind, A. P. (1966) Über den Einfluss von Feuchtigkeitsänderungen auf das Kriechen von Buchenholz quer zur Faser unter Berücksichtigung von Temperatur und Temperaturänderungen, Holz als Roh- und Werkstoff, vol. 24, p.87-97.